Nichtlineare Optik

Michael Kuron[1] and Henri Menke[1]
(Betreuer: Xinghui Yin)
Gruppe M24

(08/04/2014)

The laser, which wasn't invented until the early 1960s, has quickly become a standard tool found not only in most physics laboratories around the world today, but also as part of everyday consumer technology: information storage on compact discs, cutting and etching in industrial production, precision measurement, medical instruments and a multitude of other applications would be a great deal more difficult without this ingenious technology.

While the original helium-neon laser only produced red light at 633 nm, many applications called for the availability of more colors. One method to get there is the application of linear optics: Some crystals can lase in the near-infrared when pumped by an appropriate light source and placed inside a resonator cavity; in this way, an Nd:YAG crystal can produce 1064 nm light. To get this down into the visible spectrum, the non-linear effect of frequency doubling is applied. A KTP crystal reduces this wavelength to green 532 nm.

Another non-linear optical effect that can be used to improve laser efficiency is Q-switching: here, a crystal whose transparency depends on the incident light intensity can switch the laser resonator between two states which causes light to be emitted in pulses.

CONTENTS

I. THEORETICAL BASICS

A. The Laser Principle

The word Laser is an acronym for *Light Amplification by Stimulated Emission of Radiation*. The mechanism to achieve such an amplification was derived in 1917 by Einstein in form of Planck's law of radiation. In general, a Laser is consists of a two-level system. As the acronym already suggests, it works on top of stimulated emission and absorption.

1. Photon Model of a Single Mode Laser

Often the Laser principle is described by means of a semi-classical theory which allows to derive pump thresholds where lasing is possible. Unfortunately this description is incomplete as we clearly observe emission of radiation below the threshold.

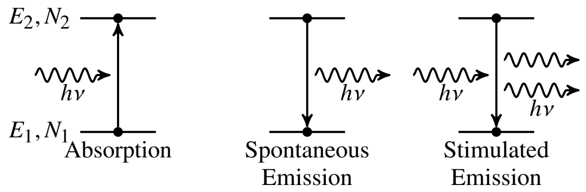

FIG. 1. The different transition processes between the two levels of energies E_1 and E_2. The transition energy is given in $h\nu$. Above the higher level, the corresponding Einstein coefficient is noted.

Light is spontaneously emitted by excited atoms, hence a classical description of the electro-magentic field is not applicable for this emission only occurs when the two-level system couples to an external field. The other processes involved are absorption and stimulated emission. We will discuss these processes for a two-level system in thermodynamic equilibrium.

The full quantum mechanical description of the Laser is tedious and the population $n(t)$ of the levels should be an integer. For the sake of simplicity, we will assume $n(t)$ to be continuous and won't derive expression for the transition rates. Also we assume $n(t)$ to contain only one distinct set of photon (i.e. those with wavelength λ). The quantum theory of Laser is described in detail in, e.g. Haken [1].

As displayed in Figure 1 there are three processes to be considered. These processes happen with a certain probability. Then the processes are quantified by the following rate equations (more thoroughly described in Haken [1], Haken and Wolf [2]):

Absorption: This is the process of absorbing one photon from the external field to reach an energetically higher state; for a two-level system this is the excited state. Hence the dynamics of the population is proportional to the radiation density of the field.

$$\mathrm{d}n_1 = -N_1 W n \,\mathrm{d}t. \tag{1}$$

The coefficient W corresponds to the number of photons a single atom absorbs/emits per second.

Spontaneous Emission: This process is independent from the light field. The excited state decays to the ground state by emission of a photon.

$$dn_2 = N_2 W \, dt. \tag{2}$$

Stimulated Emission: Instead of the photon being absorbed by the ground state, it can also trigger a radiating decay of the excited state. This is again dependent on the radiation density.

$$dn_3 = N_2 W n \, dt. \tag{3}$$

This is analogous to the absorption process.

Loss Rate: Because the photons are not contained within the cavity but can leave it through a translucent mirror or can be scattered at impurities, we need to take into account a loss of photons. Let therefore $\kappa = 1/t_1$ be the inverse of the lifetime of the photons.

$$dn_4 = -2\kappa n \, dt. \tag{4}$$

All these processes happen simultaneously. In thermodynamic equilibrium the condition of *detailed balance* demands

$$dn = \sum_{i=1}^{4} dn_i \tag{5}$$

Because the probability for spontaneous emission is tiny compared to the others, it will be neglected in the following text. Hence we obtain the following rate equation:

$$\frac{dn}{dt} = (N_2 - N_1)Wn - 2\kappa n \tag{6}$$

Not only the number of photons changes during the transition process but also the populations of the atomic levels. In a later section the concept of pumping will be introduced. For now it shall suffice that there is a pump rate w_{ij} which describes the number of electrons which are transferred from level j to i by pumping.

$$\frac{dN_1}{dt} = w_{12}N_2 - w_{21}N_1 + (N_2 - N_1)Wn, \tag{7a}$$

$$\frac{dN_2}{dt} = w_{21}N_1 - w_{12}N_2 - (N_2 - N_1)Wn. \tag{7b}$$

The number of atoms in the active medium is assumed to be nearly constant, hence $N = N_1 + N_2$. We introduce the quantity of *inversion*[1] $D \equiv N_2 - N_1$. With some approximations and the quantities

$$\frac{1}{T} = w_{21} - w_{12}, \quad D_0 = N\frac{w_{21} - w_{12}}{w_{21} + w_{12}}, \tag{8}$$

the time-dependent Laser equation can be derived[1]

$$\frac{dn}{dt} = (D_0 W - 2\kappa)n - 2D_0 T W^2 n^2. \tag{9}$$

Considering the stationary limit of (9), i.e. $n = n_0$ the Laser condition can be derived

$$D_0 W - 2\kappa > 0. \tag{10}$$

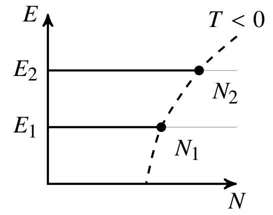

FIG. 2. Energy scheme of a two-level system for the case of population inversion: The population of the excited state is greater than the one of the ground state. The dashed line corresponds to a Boltzmann distribution with negative temperature.

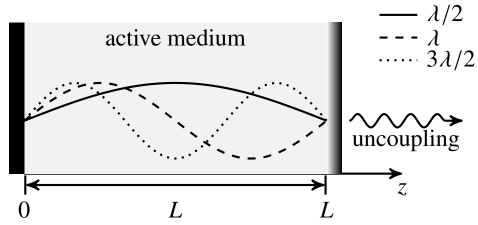

FIG. 3. Sketch of a cavity. The cavity is bounded by two mirrors, the one on the right hand side is semi-transparent. Early lasers used a mixture of He and Ne gas for the active medium. Examples for fitting wave lengths are also sketched with solid, dashed and dotted lines.

2. Population Inversion

Because the states are populated according to the Boltzmann distribution, the ground state population will be greater than the excited state population:

$$N_1 > N_2. \tag{11}$$

It follows that emission processes are unlikely due to the unfortunate population gradient with regard to the excited state; i.e. A_{21} and B_{21} are small. To get the system into a lasing state, the population gradient needs be reversed, hence the populations need to be inverted.

$$N_1 < N_2. \tag{12}$$

By the thermodynamical definition of temperature, this population inversion can be interpreted as a negative absolute temperature, see Figure 2.

The main idea of a laser is to artificially create such a population inversion in an active medium enclosed in a cavity.

3. Experimental Realisation

The cavity mentioned before is normally built by using two mirrors where one is selectively translucent. Selection is done with regard to the frequency of the incident light beam on the mirror. To ensure a constant beam the population inversion needs to be maintained. This is done by pumping the excited state either with an external driving light source or (in our case) by using the light which is reflected by the translucent mirror.

The process important for lasing is the stimulated emission. Also the nonzero probability of spontaneous emission is neglected.

Due to the finite lifetime of a state, the line of the emitted light is broadened. Normally this broadening would occur with

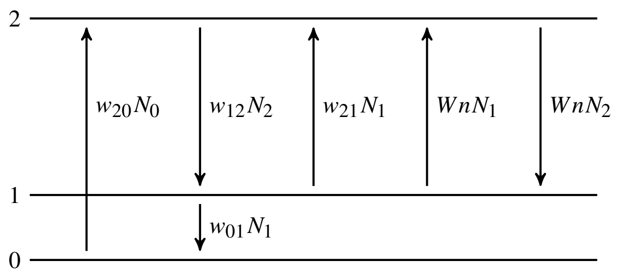

FIG. 4. Transition scheme in a three-level system in which optical transitions take place from the highest to the middle level.

a Gaussian profile. Because the active medium is enclosed in a resonator which only allows discrete modes with the boundary conditions $2L = k\lambda$ ($k \in \mathbb{N}$), the profile can only be described by a Lorentzian. If the output coupling is limited to a single wave length, we can create a *single mode Laser* with a sharp single emission line.

4. Relaxation Oscillations

By the example of a three-level Laser we will show that n and N_j perform damped oscillations as illustrated in Figure 4. We assume that the transition $1 \rightarrow 0$ is fast. Using $D = N_2 - N_1$ and $N = \sum_{i\in\{0,1,2\}} N_i$, the Laser equations for this system read

$$\begin{aligned} \frac{\mathrm{d}n}{\mathrm{d}t} &= -2\kappa n + DWn, && \text{(photons)} \\ \frac{\mathrm{d}N_2}{\mathrm{d}t} &= Nw_{20} - w_{12}N_2 - WN_2 n. && \text{(populations)} \end{aligned} \tag{13}$$

As already stated, the transition from $1 \rightarrow 0$ is fast, hence the population N_1 will decay faster than other populations can decay into this level. Thus N_1 is negligible and $D \approx N_2$. We now consider small deviations of D and n:

$$D = N_2^0 + \delta N_2, \quad n = n_0 + \delta_n. \tag{14}$$

Differential equations for δN_2 and δn can be derived and solved with the ansatz $A\exp(\alpha t)$. This yields

$$\alpha = -\Gamma + \mathrm{i}\omega_r. \tag{15}$$

This means that the deviation from a stationary population is oscillating with ω_r and decaying with Γ. This makes the general solution for the deviation of the photon number

$$\delta n = A_1 \mathrm{e}^{-(\Gamma - \mathrm{i}\omega_r)t} + A_2 \mathrm{e}^{-(\Gamma + \mathrm{i}\omega_r)t}. \tag{16}$$

5. Transformation of the Rate Equations

According to section IV of the manual[3], the rate equations can be transformed to quantities that are easily measurable:

$$\begin{aligned} \frac{\mathrm{d}g}{\mathrm{d}t} &= -\frac{g - g_0}{\tau_L} - \frac{gP}{E_{\mathrm{sat}}}, \\ \frac{\mathrm{d}P}{\mathrm{d}t} &= \frac{2g - \ell}{T_R} P + \frac{2g}{T_R} P_{\mathrm{vac}}. \end{aligned} \tag{17}$$

The following definitions were used:

- g: Cycle gain
- $g_0 = \frac{\sigma_L}{2A_{\mathrm{eff}}} R\tau_L$: Small-signal gain
- τ_L: Lifetime of the excited Laser level
- $P = IA_{\mathrm{eff}}$: Radiation power
- $E_{\mathrm{sat}} = h\nu \frac{A_{\mathrm{eff}}}{\sigma_L}$: Saturation energy
- ℓ: Loss by output coupling
- T_R: Cycle time
- $P_{\mathrm{vac}} = \frac{h\nu}{T_R} \approx 0$: Vacuum fluctuation
- $A_{\mathrm{eff}} = \pi\omega_L^2$: Mode cross section in the active medium

B. Gaussian Optics

1. Low-Order Modes

The *Gaussian beam* is a special E-field solution with the intensity profile of a Gaussian. This beam can be derived by solving either the paraxial wave equation or the Fresnel-Kirchhoff integral in the Fresnel approximation. The latter approach yields a first ansatz for the Gaussian beam[4]:

$$u(x,y,z) \sim \exp\left[-\mathrm{i}k\frac{x^2+y^2}{2q}\right], \tag{18}$$

where $k = \omega/c$ is the familiar wave number and $q = q(z)$ is the complex beam parameter. Considering the free space solution (no limitation in z-direction) one has[4]

$$u(x,y,z) = u_0 \frac{w}{w_0} \exp\left[\frac{x^2+y^2}{w^2}\right] \exp\left[-\mathrm{i}k\frac{x^2+y^2}{2R}\right] \exp[\mathrm{i}\phi], \tag{19}$$

with $w = w(z)$, $R = R(z)$ and $\phi = \phi(z)$ being the geometry parameters of the beam.

Because the intensity is proportional to the square of the field, $I \sim |E|^2$, it can be expressed as

$$I(x,y,z) = I_0 \left(\frac{w}{w_0}\right)^2 \exp\left[2\frac{x^2+y^2}{w^2}\right]. \tag{20}$$

Now that all important quantities have been defined, we will investigate the geometry parameters and their effect on the beam profile. Before we begin, we need definition of the *Rayleigh range*[4]

$$z_R = \frac{\pi\omega_0^2}{\lambda}. \tag{21}$$

Transverse profile: As is obvious from (19), the transverse profile is a Gaussian with a width of $w(z)$. The width is given by

$$w(z)^2 = w_0^2\left(1 + \frac{z^2}{z_R^2}\right). \tag{22}$$

This expression immediately reveals that the beam has its waist at $z = 0$. Do get $w(z)$ one needs to take the root, which two branches correspond to the limits of the beam.

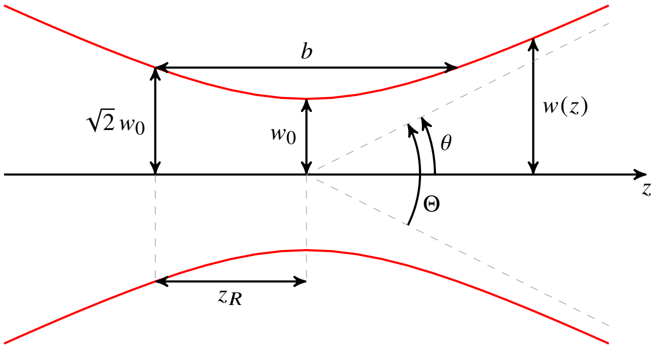

FIG. 5. Sketch of the basic parameters of a Gaussian beam. See the text for detailed explanations.

Rayleigh range and confocal parameter: In a distance from the centre equal to the Rayleigh range of the beam, the width equals

$$w(\pm z_R) = \sqrt{2}\, w_0. \tag{23}$$

The distance between z_R and $-z_R$ is called confocal parameter:

$$b \equiv 2z_R = \frac{2\pi w_0^2}{\lambda}. \tag{24}$$

Radius of curvature: The shape of the wave fronts is defined by the exponential function with imaginary exponent. The curvature of said wave fronts is defined by the radius of curvature

$$R(z) = z\left(1 + \frac{z_R^2}{z^2}\right). \tag{25}$$

Divergence: Half of the opening angle of the Gaussian beam is defined as the divergence

$$\theta = \frac{\Theta}{2} = \arctan\left(\frac{w_0}{z_R}\right) = \arctan\left(\frac{\lambda}{\pi w_0}\right), \tag{26}$$

i.e. the smaller b, the wider the opening angle and hence the larger the divergence.

Gouy phase: This describes the on-axis longitudinal phase delay and is defined as

$$\phi(z) = \arctan\left(\frac{z}{z_R}\right). \tag{27}$$

2. *Higher-Order Modes*

As already stated, the Gaussian beam is just an approximation. It is also possibly to find more general solutions to the paraxial wave equation. It can be derived[4] that the *Hermite-Gaussian modes* are also eigensolutions. In this case the Gaussian is multiplied with the Hermite polynomials H_n with $n \in \mathbb{N}$. For reference, this general form is

$$\begin{aligned} u_{\ell,m}(x,y,z) = u_0 \frac{w}{w_0} H_\ell &\left[\sqrt{2}\frac{x}{w(z)}\right] H_m \left[\sqrt{2}\frac{y}{w(z)}\right] \\ &\times \exp\left[\frac{x^2+y^2}{w^2}\right] \exp\left[-\mathrm{i}k\frac{x^2+y^2}{2R}\right] \\ &\times \exp[\mathrm{i}(1+\ell+m)\phi]. \end{aligned} \tag{28}$$

This result is relevant for asymmetric resonators where higher modes with $\ell, m \neq 0$ can appear.

In the special case of $\ell = m = 0$ ($H_0 = 1$) we obtain the normal Gaussian beam described in the previous text.

C. Optical Resonators

Besides the active medium, the resonator is an important component of the Laser. The resonator ensures that the beam crosses through the active medium many times, increasing the intensity. Also the geometry acts in a frequency selecting way, because not all modes "fit" into the resonator.

In most cases the Laser resonators consists of two facing mirrors—one of these is semi-transparent—with the active medium enclosed in between.

For the resonator to work in the way described above, some conditions need to be met. For low loss, only a small number of beams may leave the resonator at the sides. Else all the intensity will vanish.

Not every resonator can contain stable modes. For stable modes to exist, the *stability condition* has to be met: Consider therefore an arbitrary two-mirror resonator of length L with curved mirror with the radii of curvature R_1 and R_2. Using two rays and the cavity round trip matrix, it can be derived[4] that

$$0 < \underbrace{\left(1 - \frac{L}{R_1}\right)}_{\equiv g_1}\underbrace{\left(1 - \frac{L}{R_2}\right)}_{\equiv g_2} < 1. \tag{29}$$

D. Second Harmonic Generation

In vacuum the description of electrodynamics by the Maxwell equations can be considered complete. If the field interacts with matter this microscopic approach isn't suitable. Instead, the response of the medium is described by the electric susceptibility χ which is associated with the polarisation $\boldsymbol{P}$:

$$\boldsymbol{P} = \varepsilon_0 \sum_n \chi_n \boldsymbol{E}^n = \varepsilon_0\chi_1\boldsymbol{E} + \varepsilon_0\chi_2\boldsymbol{E}^2 + \varepsilon_0\chi_3\boldsymbol{E}^3 + \cdots. \tag{30}$$

As the medium is not necessarily isotropic, the χ are generally tensors and the multiplications are tensor contractions.

In the Lorentz oscillator approximation, all terms containing $\boldsymbol{E}^n$ with $n \geq 2$ are neglected, i.e. this is a linear approximation. In our case however, we are interested in the first order of nonlinear effects to get *second harmonic generation* (SHG).

To achieve second harmonic generation with a Laser light source, a nonlinear crystal is placed in the beam. Diffraction causes waves of double (or half) frequency to emerge.

To show an example for the second harmonic generation, consider the following wave

$$E(t) = E_0\, \mathrm{e}^{\mathrm{i}(\omega t - kz)} + \text{c.c.}, \tag{31}$$

with $k(\omega) = \frac{\omega}{c} n(\omega)$. According to (30) we now compute the second order contribution to the polarisation.

$$|\boldsymbol{P}_2| = \varepsilon_0\chi_2 E^2 = \varepsilon_0\chi_2\left[E_0^2\, \mathrm{e}^{\mathrm{i}(2\omega t - 2kz)} + \text{c.c.}\right]. \tag{32}$$

This is obviously a polarisation wave oscillating at 2ω and a propagation constant $2k$. To avoid destructive interference with

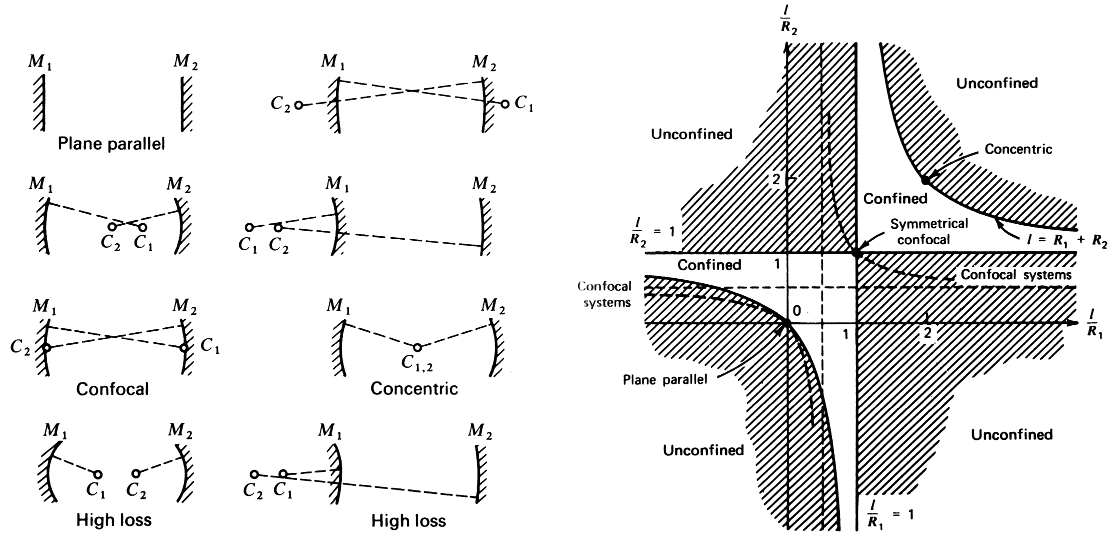

FIG. 6. Left:[5] Different kinds of cavities. Except for those in the lowermost row, all configurations enclose stable modes. Right:[5] Visual representation of the confinement condition (29). In the unshaded areas the resonator is stable.

other partial waves the second harmonic wave should have the same phase velocity, i.e.

$$k(2\omega) \stackrel{!}{=} 2k(\omega) \implies n(\omega) \stackrel{!}{=} n(2\omega). \tag{33}$$

There a two ways to place the nonlinear crystal for second harmonic generation:

Outside: The crystal is placed into the beam outside of the optical resonator. Using a lens, the beam is focused onto the crystal. This external conversion doesn't modify the resonator itself and hence has no effect on its stability.

Inside: A nonlinear crystal is placed between the active medium and the resonator mirrors, i.e. inside the cavity. Thus the beam is automatically focused. The crystal introduces an additional loss term in the rate equations. The output coupling of the second harmonic wave can be done using the selectivity of the mirrors and the cavity properties. The advantage over the other placement is that the beam now has the full intensity. A drawback is that the resonator stability will suffer.

E. Q-Switch

Under *continuous wave mode* (cw) operation, the population inversion gets clamped to its threshold value. Even during *pulsed operation*, the population inversion exceeds this threshold by only a small amount. But in the pulsed mode the intensity is inversely proportional to the duration of the pulse τ. The generation of those pulses is done via *resonator quality (Q) switching*; one distinguishes between active and passive Q-switching.

Passive: An absorbing crystal with intensity-dependent absorption coefficient is placed inside the cavity. When the active medium is pumped, the population of photons—and hence the intensity—increases. Eventually a certain threshold is reached and the absorber becomes transparent and the pulse is radiated off. Simultaneously, the population decreases and the absorber becomes opaque again, i.e. only a short pulse is emitted.

Active: An active Q-switch is placed outside of the cavity. One way of switching the beam on and off is by using a rotating mirror or prism. Unfortunately the speed of rotation is very limited for these mechanical devices and results in relatively slow Q-switching.

II. EXPERIMENTAL PROCEDURE

Figure 7 shows the experimental setup used. It consists of a 808 nm laser as pumping light source, which is focussed by two lenses onto the Nd:YAG crystal which is coated with a planar mirror on this side. At the other end of the resonator cavity, mirrors with different transmittivities (0, 10, 20, 30 %) can be placed. Inside the cavity, a KTP crystal or an Cr:YAG crystal can be placed (not shown). The light coupled out of the cavity is focussed by another lens and picked up by either an intensity meter, a photo diode, or the wall at the far end of the table as illustrated in the picture. The last lens may also be used to focus the light onto the KTP crystal before it is picked up by one of the detectors.

To start out, the 10% output coupling (OC) mirror is mounted at the far end of the resonator, which should be slightly less than 0.10 m in length. The pumping laser is turned on and the position of the OC mirror is varied until laser operation commences. This can be detected by holding a IR fluorescence card right after the OC mirror. As the card starts to burn almost immediately, fine adjustments are made using the power meter to optimize the output power.

This process is performed for all three OC mirrors and a number of different currents applied to the pumping light source. Next, the resonator length is varied for the 10% mirror and a high current.

The second task consists of frequency-doubling the laser into the green by placing the KTP crystal at the focus of the final lens. Optimization of the laser can now be performed by looking at the brightness of the green spot on the wall. Another parameter that should be optimized is the KTP crystal's angle of rotation. This time, the power meter is used to determine the green output power for various currents applied to the pumping

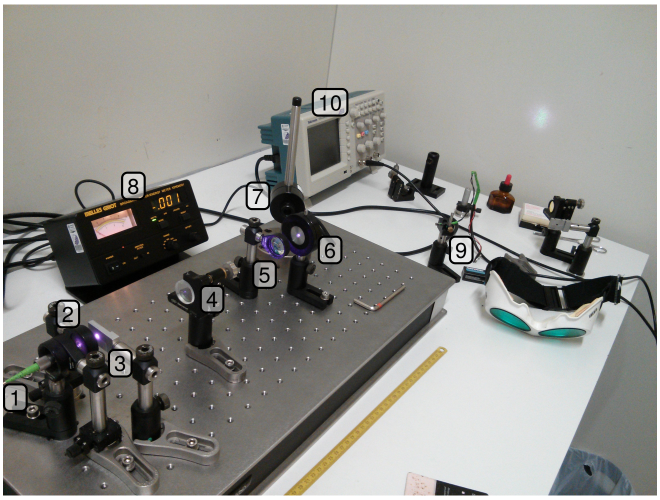

FIG. 7. Experimental setup. 1 Pumping Laser; 2 Lens to focus beam on the 3 Nd:YAG crystal with integrated mirror; 4 exchangeable mirror; 5 Lens; 5 KTP crystal; 7 Intensity sensor; 8 Power metre; 9 Photo diode; 10 Oscilloscope.

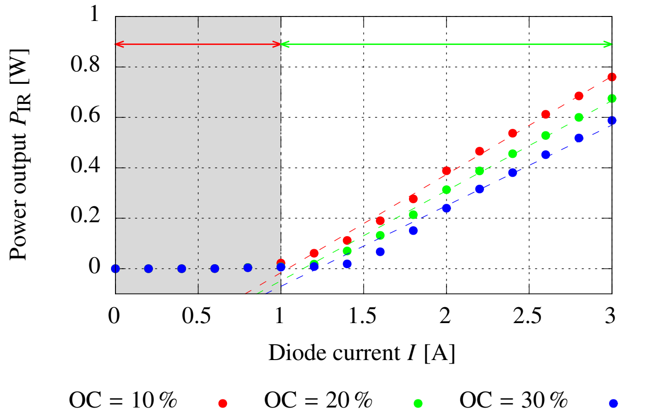

FIG. 8. Power output dependent on current applied to the pumping light source. Various degrees of OC were used, while the resonator length was kept at a constant 0.0915 m. For low currents, the laser does not operate, while for larger currents stable operation can be sustained. In this and most of the subsequent figures the stable regime is marked with a green arrow while the unstable regime is denote by a red arrow.

OC [%]	I_{start} [A]	$P_{IR}(I = 3\,A)$ [W]
10	1.041	0.760
20	1.134	0.675
30	1.220	0.588

TABLE I. Power output at which lasing commences and maximum power output, depending on the level of OC.

light source.

By placing the Cr:YAG crystal into the resonator, the brightness of the green spot on the wall should increase dramatically. The KTP crystal is now removed and as before, the laser output power is optimized. Again, the output power as is measured for various currents applied. Now, the power meter is replaced with the photo diode hooked up to the oscilloscope. After making sure that the oscilloscope signal does not clip due to saturation of the diode (if it does, the photo diode can be rotated slightly to reduce the amount of incident light), the oscilloscope can be used to resolve individual pulses and their duty cycle and period can be determined. This time, the pulse frequency should be determined for various currents applied to the pumping source.

Finally, the Cr:YAG crystal is replaced with the KTP crystal and the 0% OC mirror is mounted. As before, the OC mirror is positioned to optimize the brightness of the green spot on the wall. If necessary, the KTP crystal's rotation can also be optimized. In this setup, the green output intensity is also measured for various applied currents.

III. ANALYSIS

A. Parameters of the Laser

To start out, various parameters of the continuous wave Nd:YAG laser were varied to determine how they influence its output power.

Figure 8 shows the dependency on the current I applied to the pumping light source for three different degrees of OC. The lasing starts at a current of roughly 1 A; the exact starting point increases slightly when increasing the OC and is listed in Table I as determined by fitting a linear function to the ascending part of the graph. As we do not know the characteristic of the pumping light source, there is not necessarily a linear relation between diode current and pumping intensity, so no quantitative statements about the laser's dependency on pumping intensity can be made.

It is clearly visible from Table I that for OC = 10 %, the laser starts at the lowest pumping intensity and reaches the highest power at the final maximum intensity. Both appear to depend on the OC in a roughly linear fashion.

The optimal OC can be determined from the rate equation (17). In stationary operation ($\dot{P}(t) = \dot{g}(t) = 0$) and with negligible vacuum fluctuations ($P_{vac} = 0$), these reduce to

$$0 = -\frac{g - g_0}{\tau_L} - \frac{gP}{E_{sat}} \text{ and } g = \frac{\ell}{2}. \tag{34}$$

Plugging in $\ell = -\ln(1-\mathrm{OC})-\ln(1-s)$ as given in the manual[3] and solving for the output power

$$P_{out} = \mathrm{OC} \cdot P = -\frac{E_{sat} \cdot \mathrm{OC}}{\tau_L}\left(\frac{2g_0}{\ln(1-\mathrm{OC}) + \ln(1-s)} + 1\right) \tag{35}$$

allows for optimization with regard to the output power. For our laser's parameters, $g_0 = 0.9$ and $E_{sat} = 2 \cdot 10^{-4}$ J, while $s = 1 - 2\,\%$ is estimated. This gives us an optimal OC = $9 - 12\,\%$.

Next, the resonator length was varied; the dependency of the output power for a fixed OC and I is shown in Figure 9. It is clearly visible that the laser is stable at a largely constant output power up to a length of 0.10 m, at which point the stability condition (29) is violated. The weak dependency on the actual length is due to the fact that the length of active medium (the crystal) is not varied.

The left mirror was planar, the right one had a focal length of 50 mm. This corresponds to $R_1 = \infty$ and $R_2 = 100$ mm, which gives us $L \in [0, 0.10]$ m, a requirement which was confirmed in experiment.

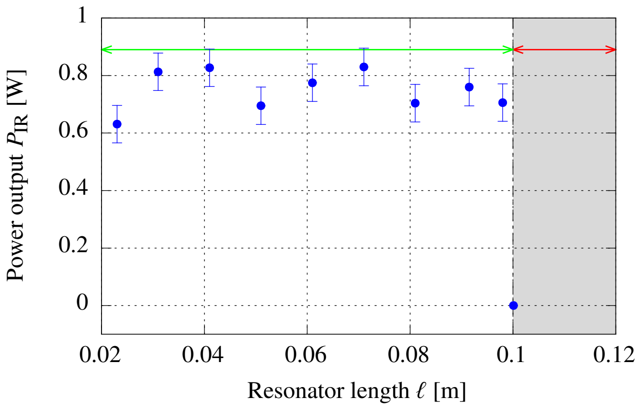

FIG. 9. Power output dependent on the resonator length with a diode current of $I = 3.0\,\mathrm{A}$ and an OC = 10 %. The error bars represent the standard deviation of the mean value in the stable regime.

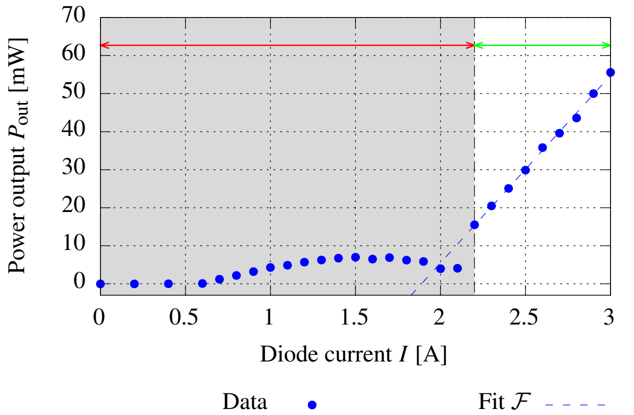

FIG. 10. Power output for the second harmonic generation with external KTP crystal.

B. External Second Harmonic Generation

Up to this point, the laser operated in the infrared. To shift it into the visible green spectrum, the KTP crystal was placed at the focus of the output beam and rotated until the green spot on the wall was brightest. KTP is a birefringent crystal with two different indices of refraction along its two axes; rotating the crystal chooses a different balance of these two indices of refraction so that at the optimum, the condition (33) was met.

In Figure 10, the dependency of the output power of the green light on the pumping light source current is shown. The laser does not pick up stable operation until a pumping current of 2.2 A is reached. This is due to the SHG crystal requiring a certain minimum amount of incident infrared light before it picks up stable operation.

C. Q-switching the Laser

To passively switch the quality of the laser resonator between a high and a low value, the Cr:YAG crystal was placed inside the resonator. This immediately increased the brightness of the green dot by a significant amount. To compare with previous data, the KTP crystal was removed again and the resulting

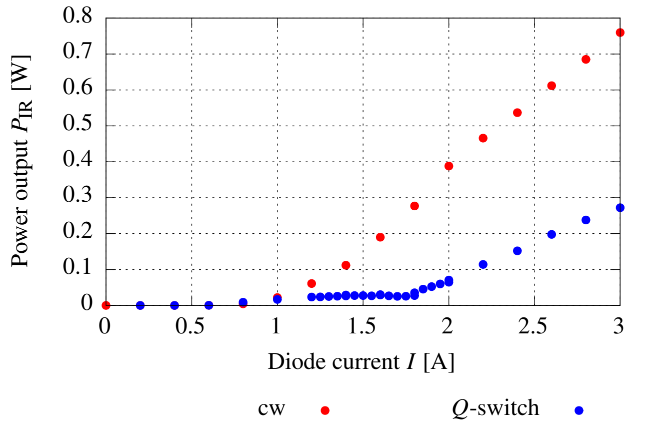

FIG. 11. Power output dependent on the diode current with Q-switching turned on. This is compared with the continuous-wave results from Figure 8. Both curves were recorded with OC = 10 % and a resonator length of 0.0915 m.

dependency of the output power on the pumping light source current is shown in Figure 11. It is clearly visible that the output power of the Q-switched laser is in no way greater than that of the cw laser. However, the maximum intensity of each pulse is significantly higher than the intensity of the cw laser. This is not resolved by the power meter which is not sensitive on the time scale of the pulse rate, so technically the points on the graph show the average intensity of the Q-switched laser.

Another point worth noting is the high intensity of the green light: evidently, the KTP crystal's intensity depends on the power of the incoming IR light in a nonlinear way so that the green emission near the peak of the pulse is very large compared to that during continuous operation, large enough to dominate it even when averaging over the entire pulse period.

With Q-switching, the laser does start lasing at the same point (near 1 A) as without, but the output power stays mostly constant up to another point (near 1.8 A).

The pulse shape is shown exemplarily in Figure 12. It was recorded by attaching a high-speed photo diode to an oscilloscope. To get an impression of the maximum intensity of the pulse, a numerical integration over one pulse period was performed to obtain the mean intensity; the quotient of peak to mean intensity turned out to be roughly 15 for the pulse shown there (it was lower for higher repetition frequencies), which makes the maximum Q-switch output power several times greater than the continuous cw output power.

Another property of the Q-switched that could be determined using the photo diode the is the pulse rate, or its inverse, the repetition frequency. It varies with the applied pumping laser intensity as shown in Figure 13. The cause of this dependency is obvious as higher pumping intensities cause the inversion state to be reached after a shorter time. For very small pumping intensities, inversion is never reached, which explains the existence of the second characteristic point in Figure 11. Between the point where cw lasing sets in and this point where the SHG sets in, only little emission occurs with a weak dependency on the current applied to the pumping light source.

While the repetition frequency starts out with a linear dependency on the current applied to the pumping source, the curve tends to flatten off. Again, as we don't know the characteristic of the pumping light source, no quantitative arguments can be

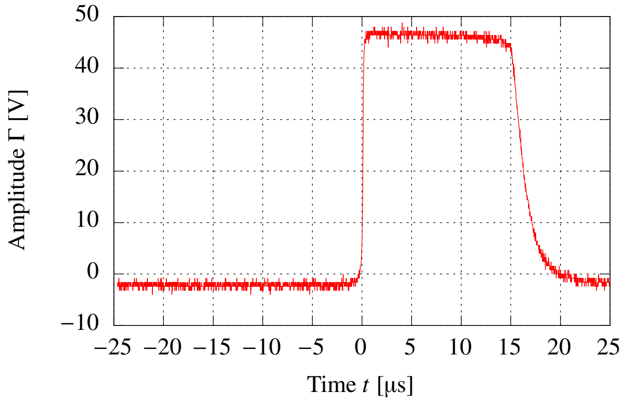

FIG. 12. Peak shape of the Q-switched laser operation.

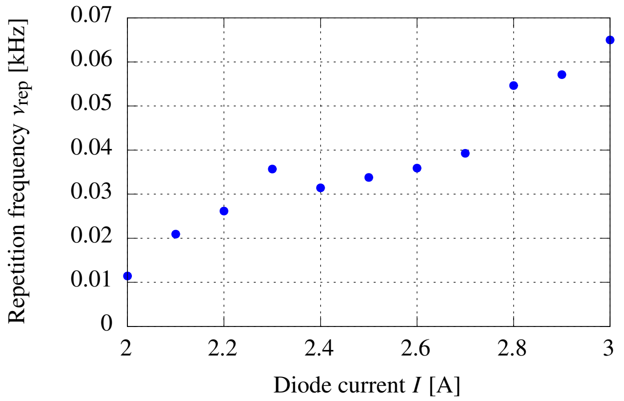

FIG. 13. Repetiton frequency for the Q-switched laser with OC = 10 % and a constant resonator length of 0.0915 m.

made, but it can be speculated that the repetition frequency eventually saturates for larger pumping intensities. This could be explained by the time it takes the absorbing crystal to relax from the transparent back to the absorbing state; this time scale might be on the order of 0.01 s.

D. Internal Second Harmonic Generation

After removing the Q-switching crystal, the KTP crystal is placed back into the setup, this time inside the resonator. Figure 14 shows the dependency of the output intensity on the current applied to the pumping light source. Comparing this graph with the one obtained with external SHG, Figure 10, shows that stable operation sets in much earlier, at only 0.6 A. Also, the output power reached at the highest applied current is nearly twice what it was before. It should be noted that the power meter's reading fluctuated strongly (sometimes by up to 50% over the course of a few seconds), so the inertia-averaged analog reading was used instead of the instantaneous digital meter output. Clearly, internal SHG is favorable in terms of efficiency. At the same time however, the resonance becomes unstable at higher pumping intensities and the output power fluctuates strongly on macroscopic timescales.

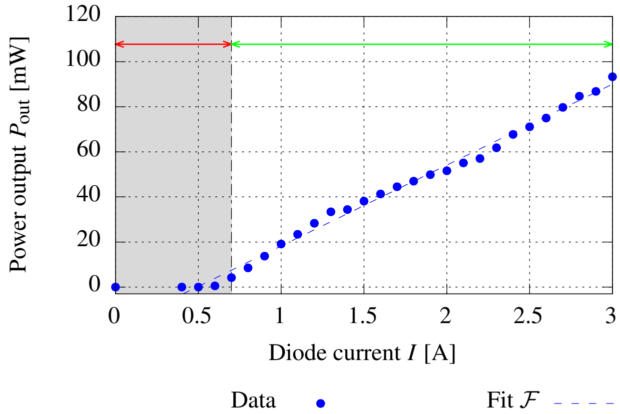

FIG. 14. Power output for the second harmonic generation with intra-cavity KTP crystal.

IV. SUMMARY

An infrared laser was successfully constructed from simple optical elements and a mirror-coated Nd:YAG crystal. Various levels of output coupling and pumping intensity were tested and the resonator length was varied. This confirmed the theoretical length requirements in experiment. The laser intensity did not depend on the resonator length beyond the breakdown upon violating the stability condition. OC near 10% was found to be favorable for maximum output power. Once the pumping intensity was sufficient to get the lasing started, the output power depended mostly linearly on the current applied to the pumping light source, whose power-current characteristic was unknown and thus no actual quantitative arguments could be made about the pumping intensity.

Next, an external KTP crystal was used to frequency-double the infrared light into green light.

By adding a Cr:YAG crystal as a passive Q-switch into the resonator, the laser was modified to output pulses instead of continuous waves, which greatly increased the apparent brightness of the green light. While the average infrared output intensity of the laser has decreased by Q-switching, the peak intensity of each pulse is now multiple times of the cw value.

Lastly, the laser was returned back to cw operation and the KTP crystal inserted into the resonator. This allowed the lasing to commence at a lower pumping intensity and reached a maximum green output intensity of almost twice its previous value, while coming at the cost of making the resonator unstable for large pumping intensities.

REFERENCES

[1] H. Haken, *Licht und Materie, Band 2: Laser*, 2nd ed. (BI-Wissenschaftsverlag, 1995).

[2] H. Haken and H. C. Wolf, *Atom- und Quantenphysik*, 8th ed. (Springer Verlag, 2004).

[3] Universität Stuttgart (Hrsg.), *Fortgeschrittenenpraktikum: Versuchsanleitung*, Universität Stuttgart (2014).

[4] O. Svelto, *Principles of Lasers* (Springer, 2010).

[5] A. Yariv, *Quantum electronics* (Wiley, 1989).